Plant Disease • 2025 • 109:770-778 • https://doi.org/10.1094/PDIS-10-24-2111-SR

Special Report

Eight Novel Diagnostic Markers Differentiate Lineages of the Highly Invasive Myrtle Rust Pathogen *Austropuccinia psidii*

Zhenyan Luo,[1] Jinghang Feng,[1] Austin Bird,[1] Mareike Moeller,[1] Rita Tam,[1] Luc Shepherd,[1,2] Lydia Murphy,[1] Lavi Singh,[1] Abigail Graetz,[1] Lilian Amorim,[3] Nelson Sidnei Massola Júnior,[3] M. Asaduzzaman Prodhan,[2] Louise Shuey,[4] Douglas Beattie,[5] Alejandro Trujillo Gonzalez,[6] Peri A. Tobias,[7] Amanda Padovan,[1] Rohan Kimber,[8] Alistair McTaggart,[9] Monica Kehoe,[2] Benjamin Schwessinger,[1,†] and Thaís R. Boufleur[1,3,†]

[1] Research School of Biology, The Australian National University, Canberra, ACT 2601, Australia
[2] DPIRD Diagnostics and Laboratory Services, Department of Primary Industries and Regional Development, South Perth, WA 6151, Australia
[3] Department of Plant Pathology and Nematology, Luiz de Queiroz College of Agriculture, University of São Paulo, Piracicaba, SP 13418-900, Brazil
[4] Queensland Department of Agriculture and Fisheries, Ecosciences Precinct, Dutton Park, QLD 4102, Australia
[5] Office of the Gene Technology Regulator, Evaluation Branch Australian Government, Department of Health and Aged Care, Scarborough House, Atlantic St, Phillip, ACT 2606, Australia
[6] Centre for Conservation Ecology and Genomics, Institute for Applied Ecology, University of Canberra, Bruce, ACT, Australia
[7] School of Life and Environmental Sciences, Faculty of Science, The University of Sydney, Camperdown, NSW 2006, Australia
[8] Crop Sciences, South Australian Research and Development Institute (SARDI), Waite Research Precinct, Urrbrae, SA 5064, Australia
[9] Centre for Horticultural Science, Queensland Alliance for Agriculture and Food Innovation, The University of Queensland, Ecosciences Precinct, Dutton Park, QLD, Australia

Abstract

Austropuccinia psidii is the causal agent of myrtle rust in more than 480 species within the family Myrtaceae. Lineages of *A. psidii* are structured by their hosts in the native range, and some have success in infecting newly encountered hosts. For example, the pandemic biotype has spread beyond South America, and proliferation of other lineages is an additional risk to biodiversity and industries. Efforts to manage *A. psidii* incursions, including lineage differentiation, rely on variable microsatellite markers. Testing these markers is time-consuming and complex and requires reference material that is not always readily available. We designed a novel diagnostic approach targeting eight selectively chosen loci including the fungal mating-type *HD* (homeodomain) transcription factor locus. The *HD* locus (*bW1/2-HD1* and *bE1/2-HD2)* is highly polymorphic, facilitating clear biological predictions about its inheritance from founding populations. To be considered as potentially derived from the same lineage, all four *HD* alleles must be identical. If all four *HD* alleles are identical, six additional markers can further differentiate lineage identity. Our lineage diagnostics relies on PCR amplification of eight loci in different genotypes of *A. psidii* followed by amplicon sequencing using Oxford Nanopore Technologies and comparative analysis. The lineage-specific assay was validated on four isolates with existing genomes, on uncharacterized isolates, and directly from infected leaf material. We reconstructed alleles from amplicons and confirmed their sequence identity relative to their reference. Genealogies of alleles confirmed the variations at the loci among lineages/isolates. Our study establishes a robust diagnostic tool for differentiating known lineages of *A. psidii* based on biological predictions and available nucleotide sequences. This tool is suited to detecting the origin of new pathogen incursions.

Keywords: diagnostics, homeodomain genes, mating-type, Myrtaceae, Oxford Nanopore Technologies

Austropuccinia psidii, the causal agent of myrtle rust in more than 480 host species within the Myrtaceae family (Carnegie and Giblin 2014), is among the world's top 10 priority fungal species for biosecurity (Hyde et al. 2018). Its broad host range and rapid adaptability to new environments is a threat to biodiversity and industries (Chock 2020), especially in regions like Australia and New Zealand, where species of the Myrtaceae family are ecologically dominant and culturally important (Hyde et al. 2018). In eucalypts, for example, losses in volume because of rust severity can vary from 23 to 35% (dos Santos et al. 2020).

Initially described in Brazil (Winter 1884), *A. psidii* remained limited to the Americas for many decades before spreading to all

†Corresponding authors:
B. Schwessinger; benjamin.schwessinger@anu.edu.au,
and T. R. Boufleur; thaisboufleur@usp.br

Z. Y. Luo, J. H. Feng, and A. Bird contributed equally to this work.

B. Schwessinger and T. R. Boufleur share the last authorship.

This manuscript is preprinted at BioRXIV under https://doi.org/10.1101/2024.02.19.580897.

The author(s) declare no conflict of interest.

Funding: A. T. Gonzalez, R. Kimber, and B. Schwessinger were supported by an Australian Government grant from the Department of Agriculture, Fisheries and Forestry entitled "Automated air sampling for remote surveillance and high throughput processing of environmental samples for eDNA analyses." B. Schwessinger and P. A. Tobias were supported by an ARC Linkage grant LP190100093. São Paulo Research Foundation (FAPESP) Grant 2019/13191-5. T. R. Boufleur was supported by FAPESP Grants 2022/11900-1 and 2021/01606-6.

e-Xtra: Supplementary material is available online.

Accepted for publication 11 October 2024.

continents, except Europe and Antarctica (Simpson et al. 2006). In Australia, where the pathogen was first detected in 2010 (Carnegie et al. 2010), only the pandemic biotype (group of organisms with identical genetic constitution) has been reported, and isolates belonging to exotic lineages of *A. psidii* are considered a threat to Australian natural environments and commercial native forests (DAFF 2023; Makinson et al. 2020). Disease symptoms and spore morphology are highly similar across isolates of *A. psidii* belonging to different lineages, even in cases with strong host associations (Boufleur et al. 2023; Ferrarezi et al. 2022; Morales et al. 2024). The disease is predominantly caused by the clonal stage of the pathogen, urediniospores. It is characterized by the initial appearance of small chlorotic spots developing into bright orange pustules that generate new infective urediniospores.

Early detection and diagnosis are crucial for tracking and potentially limiting rust fungal incursions (Hussain et al. 2020). Microsatellite markers have been used to differentiate lineages of *A. psidii* (Graça et al. 2013; Stewart et al. 2018), but their application can be time-consuming and complex, particularly on a large scale. In addition, they require reference material to calibrate microsatellite profiles, which are not always readily available for *A. psidii*. The current internationally approved assay to diagnose *A. psidii* is a species-specific quantitative PCR (Baskarathevan et al. 2016; IPPC 2018); however, the choice of locus lacks the variability needed to clearly differentiate among pathogen lineages (Ahmed et al. 2018; Beenken 2017; Boufleur et al. 2023). Therefore, there is a need to identify novel target regions that precisely diagnose different lineages of *A. psidii* for faster and precise action in a biosecurity response.

Mating in fungi is controlled through genes expressed at mating-type (*MAT*) loci (Wilson et al. 2015). In rust fungi, these are two unlinked loci—one contains pheromone precursors and receptors (*P/R*) and the other contains homeodomain (*HD*) transcription factors that are closely linked via a short DNA sequence. The *HD* locus encodes *bW-HD1* and *bE-HD2* genes, which are highly multiallelic in rust fungi (Luo et al. 2024) and many other Basidiomycota (Coelho et al. 2017). These transcription factors form heterodimeric complexes between alleles and regulate cellular development during mating and the fungal life cycle (Coelho et al. 2017; Cuomo et al. 2017; Wilson et al. 2015). The analysis of *A. psidii* genomes confirmed physically unlinked, heterozygous *P/R* and *HD* loci, supporting that mate compatibility in this pathogen is governed by two multiallelic *HD* genes (*bW-HD1* and *bE-HD2*) and a biallelic *P/R* gene (Ferrarezi et al. 2022). Hence, the *HD* locus has high discriminatory power for populations owing to its high allelic diversity in rust fungi (Henningsen et al. 2024; Holden et al. 2023; Luo et al. 2024). On the other hand, different lineages can share the same *HD* alleles despite being genetically divergent (Henningsen et al. 2024; Holden et al. 2023). This indicates the need for supplemental markers to the *HD* locus to differentiate lineages based on amplicon sequencing.

The aim of this study was to develop a highly sensitive assay for the detection and identification of *A. psidii* lineages. This assay can be used for monitoring existing incursions/outbreaks and to help prevent and limit further incursions of exotic lineages. Here we introduce novel primers designed to target eight highly discriminatory loci, including the two mating-type genes (*bW-HD1* and *bH-HD2*), and six additional single-copy orthologous genes (SOGs) that further increase sensitivity and robustness of lineage calling. These primers are designed to be used in combination with long-read sequencing such as those facilitated by Oxford Nanopore Technologies (ONT).

Materials and Methods

HD locus identification and primer design

The *HD* locus of five *A. psidii* isolates was identified based on available reference genomes, including Brazilian isolates belonging to two different lineages, MF-1 (from *Eucalyptus grandis*) (PRJNA215767, GCA_000469055.2) and LFNJM1 (unpublished data) from *Syzygium jambos* (Boufleur et al. 2023), and APG1 (unpublished data) from *Psidium guajava* (Gonçalves et al. 2022), along with the Au3 isolate that belongs to the pandemic biotype (Au3_v2) (PRJNA810573, GCA_023105745.1, GCA_023105775.1) (Edwards et al. 2022), and the South African isolate Apsidii_AM, that belongs to the South African biotype (PRJNA480390, GCA_003724095.1) (McTaggart et al. 2018). The *HD* locus-containing regions were identified with BLASTx (v.2.15.0) (Johnson et al. 2008) in combination with annotated *bW-HD1* and *bE-HD2 A. psidii* genes, as described by Ferrarezi et al. (2022). As expected for the *HD* locus in dikaryotic genome assemblies, two alleles of each *bW-HD1* and *bE-HD2* gene were retrieved. The alleles of each gene (*bW-HD1* and *bE-HD2*) were aligned separately with MAFFT v.7.490 (Katoh and Standley 2013), alignment gaps were removed manually, and two Bayesian inference genealogy trees were generated with BEAST2 (Bouckaert et al. 2014), using JC69 + I + G4 (Jukes and Cantor 1969) as substitution model, with gamma shape and proportion invariant estimated. TreeAnnotator v.2.7.6 (Drummond and Rambaut 2009) was used to summarize the posterior sample of trees and visualized with FigTree (2016) v.1.4.4.

Primers were designed manually based on a multiple sequence alignment of contigs containing the *HD* alleles of the pandemic Au3_v2 lineage, the South African isolate Apsidii_AM, and the Brazilian isolate MF-1. Two pairs of degenerate primers were designed

Table 1. List of primers used in the present study

Primers	Sequence (5′–3′)	Changes	Amplicon size (bp)
HDFor2DG (forward)	ATACAGTTYAGGTTWTRGCG	C/T, A/T, A/G	~1,600
HDMR1 (reverse)	GAAAGGAAATATTGCCACT	–	
HDMF2DG (forward)	YGACCGCCTTCCTTTGAG	C/T	~1,400
HDRev2DG (reverse)	GTGTCSAAGCWACCAAAATC	C/G, A/T	
HD1_alt_fwd (forward)	AGTTGATGARGRAGTGGAAG	A/G	~2,400
HD1_alt_rev (reverse)	CCARCGATTGACTTGATCACG	A/G	
OG4974 (forward)	CAACAGCAACCGTCTCAACAG	–	~1,400
OG4974 (reverse)	ATCGGTTGAGTTAGCGCCAC	–	
OG5363 (forward)	AGCATCTAACCAAACCCCATCAC	–	~1,500
OG5363 (reverse)	ATGAGGCCGCCTAATAAGCAAG	–	
OG7071 (forward)	CGACATTCACTCCTTTGCTGGT	–	~1,700
OG7071 (reverse)	ACAATGTGAGCAAGGAACTGCT	–	
OG7530 (forward)	ACAAGAATCACTGGTGTGGAAGG	–	~1,550
OG7530 (reverse)	CTTTGAGTTACAGTTGTGCACCTG	–	
OG9632 (forward)	CGACAGGTATGGGCTAGGAC	–	~1,550
OG9632 (reverse)	AAAACTTGCTTCGACGTCCG	–	
OG9774 (forward)	TGTGACGTTTCCACCTCAGG	–	~1,600
OG9774 (reverse)	TGCCCGATTTCTCACTCCAC	–	

to amplify part of *bW-HD1* (HDFor2DG + HDMR1) and *bE-HD2* (HDMF2DG + HDRev2DG) individually, and the combination of the most forward and the most reverse primers was used to amplify the partial region of the *HD* locus spanning both *bW-HD1* and *bE-HD2* (HD1_alt_fwd/HD1_alt_rev) (Table 1). The expected amplicon size was ~1,600 and ~1,400 bp for *bW-HD1* and *bE-HD2* and ~2,400 bp for the *HD* locus.

The identification of lineage-specific loci and corresponding primer designing

To distinguish isolates that share identical alleles at the *bW-HD1* and *bE-HD2* loci, we identified SOGs with OrthoFinder v.2.5.5 (Emms and Kelly 2019) using the predicted proteomes of the individual haploid chromosome scale genome assemblies of four isolates (Au3_v2, MF-1, LFNJM1, APG1, $n = 2 \times 4 = 8$). Orthogroups containing a SOG for each haplotype were selected as candidates for additional diagnostic markers. Candidates and their corresponding 200-bp flanking regions were extracted from the genomes and aligned with ClustalO v.0.1.2 (Sievers et al. 2011). Alignments were assessed for their allelic distance and all candidates with more than six distinct alleles were retained. ClustalO v.0.1.2 was applied to reformat alignments. PrimalScheme (Quick et al. 2017) command line version v.1.4.1 was used to design primers based on multiple sequence alignments. EMBOSS primersearch v.6.6.0.0 (Rice et al. 2000) was used to confirm primers that bind to conserved regions across all alleles while ensuring uniqueness within the haploid genome assemblies to avoid off-target amplifications. Primers that could capture size polymorphisms between alleles were favored. The code used for candidate identification and primer design is available at https://github.com/ZhenyanLuo/Apsi-diagnostic.

DNA extraction and amplicon amplification

The designed primers were tested with diverse samples, including four positive controls of *A. psidii*, three single-pustule isolates (LFNJM3, LFNJM4, and LFNJRM1), five field samples (CA, CG, LFNEP1, 3.1 and SYD), and three nontarget rust species (*bW-HD1* and *bE-HD2* only see Table 2). Genomic DNA (gDNA) was extracted directly from *A. psidii* urediniospores, from infected leaf material, or from urediniospores of nontarget rust species (Table 2) with the DNeasy Plant mini kit (Qiagen) according to the manufacturer's instructions. The integrity and quality of the DNA was measured with a Nanodrop spectrophotometer (Thermo Fisher Scientific) and checked by agarose gel (0.8%) electrophoresis stained with SYBR Safe (Thermo Fisher Scientific). The DNA concentration was initially determined using the Qubit 4 (Thermo Fisher Scientific) and adjusted to 25 ng/μl for downstream analysis.

In the first round of PCR tests, the aim was to evaluate the amplification of (non-) target sequences by the designed primers followed by sequence analysis using *A. psidii* and three nontarget rust isolates (*bW-HD1* and *bE-HD2* only see Fig. 1A and B; Table 2). PCR was performed on a Mastercycler Nexus X2 thermal cycler (Eppendorf). The reaction mixture, with a final volume of 25 μl, included 5 μl of 5× reaction buffer (New England Biolabs), 0.5 μl of deoxynucleotide triphosphates (dNTPs; 10 mM), 1.25 μl of each primer (10 μM), 0.25 μl of Q5 High-Fidelity DNA Polymerase (New England Biolabs), 14.75 μl of nuclease-free water (NFW), and 2 μl (up to 50 ng) of template DNA. The PCR amplification had an initial denaturation step at 98°C for 30 s, followed by 35 cycles of denaturation at 98°C for 30 s, annealing at 58°C for 30 s, and extension at 72°C for 30 s, with a final extension step at 72°C for 2 mins. Specificity tests were run in duplicate, and PCR products were visualized on 2% agarose gel stained with SYBR Safe (Thermo Fisher Scientific).

Table 2. Description of isolates and populations and of *Austropuccinia psidii* and nontarget rusts used in this study

				Amplification[a]			Alleles			
Organism	**Code**	**Source**	**Country**	**Full locus**	***bW-HD1***	***bE-HD2***	***bW-HD1***		***bE-HD2***	
Genomes										
Austropuccinia psidii	Au3	*Agonis flexuosa*	AUS	NA	NA	NA	*bW1*	*bW2*	*bE1*	*bE2*
A. psidii	MF-1	*Eucalyptus grandis*	BR	NA	NA	NA	*bW5*	*bW6*	*bE5*	*bE6*
A. psidii	APG1 (GM1)	*Psidium guajava*	BR	NA	NA	NA	*bW1*[b]	*bW7*	*bE1*	*bE7*
A. psidii	LFNJM1	*Syzygium jambos*	BR	NA	NA	NA	*bW5*	*bW6*	*bE5*	*bE6*
A. psidii	Apsidii AM	*S. jambos*	SA	NA	NA	NA	*bW3*	*bW4*	*bE3*	*bE4*
Isolates (single-pustule)										
Austropuccinia psidii	Au3[c]	*A. flexuosa*	AUS	+	+	+	*bW1*	*bW2*	*bE1*	*bE2*
A. psidii	MF-1[c]	*E. grandis*	BR	+	+	+	*bW5*	*bW6*	*bE5*	*bE6*
A. psidii	APG1 (GM1)[c]	*Psidium guajava*	BR	–	–	+	NA	NA	*bE7*	NA
A. psidii	LFNJM1[c]	*Syzygium jambos*	BR	+	+	+	*bW5*	*bW6*	*bE5*	*bE6*
A. psidii	LFNJM3	*S. jambos*	BR	+	+	–	*bW1*	*bW7*	*bE1*	*bE7*
A. psidii	LFNJM4	*S. jambos*	BR	+	+	+	*bW5*	*bW6*	*bE5*	*bE6*
A. psidii	LFNJRM1	*S. samarangense*	BR	+	+	+	*bW5*	*bW6*	*bE5*	*bE6*
Populations (urediniospores/field samples)										
A. psidii	CA	*Plinia edulis*	BR	+	+	+	*bW8*	*bW9*	*bE8*	*bE9*
A. psidii	CG	*Eugenia dysenterica*	BR	+	+	+	*bW3*	*bW10*	*bE3*	*bW10*
Populations (infected leaves/field samples)										
A. psidii	LFNEP1	*Eugenia stipitata*	BR	+	+	+	*bW5*	*bW6*	*bE5*	*bE6*
A. psidii	3.1	*Pimenta dioica*	BR	+	+	+	*bW1*	*bW2*	*bE1*	*bE2*
A. psidii	SYD	*Melaleuca quinquenervia*	AUS	–	+	+	*bW1*	*bW2*	*bE1*	*bE2*
Nontarget rust species										
Miyagia pseudosphaeria	–	–	–	NS	NS	NA	NA	NA	NA	NA
Puccinia triticina	–	–	–	NS	NS	NA	NA	NA	NA	NA
P. graminis f. sp. *avenae*	–	–	–	NS	NS	NA	NA	NA	NA	NA
P. striiformis f. sp. *tritici*	–	–	–	NS	NS	NA	NA	NA	NA	NA
Thekopsora minima	–	–	–	–	NS	NA	NA	NA	NA	NA

[a] Conventional PCR with the three sets of primers developed in the present study. Full *HD* locus, HD1_alt_fwd (forward)/HD1_alt rev (reverse) amplifies a fragment of 2,400 kb; *bW-HD1*, HDFor2DG/HDMR1 amplifies a fragment of 1,500 kb; *bE-HD2*, HDMF2/HDRev2DG amplifies a fragment of 1,400 kb; +, positive; –, negative. "NS" is defined as nonspecific amplification in at least one of the technical replicates, "NA" as not available, "–" as no amplification, and "+" as amplification of the expected size amplicon product.

[b] Allele differs by at least 3 base pairs from other alleles.

[c] *A. psidii* and nontarget rust isolates used to confirm the specificity of the designed primers.

In the second round of PCR tests, the performance of the primers was assessed against single-spore isolates and field samples (urediniospores and infected leaves) collected in Brazil and Australia (Table 2). Identical reaction conditions, as described above, were used to amplify the *bW-HD1* and *bE-HD2* loci individually (Table 2). The amplification of *bW-HD1* and *bE-HD2* loci was performed using the same PCR conditions as for testing. For amplification of 2,400-bp amplicons spanning both *bW-HD1* and *bE-HD2*, the reaction mixture, with a final volume of 50 µl, included 10 µl of 5× reaction buffer (New England Biolabs), 1 µl of dNTPs (10 mM), 5 µl of each primer

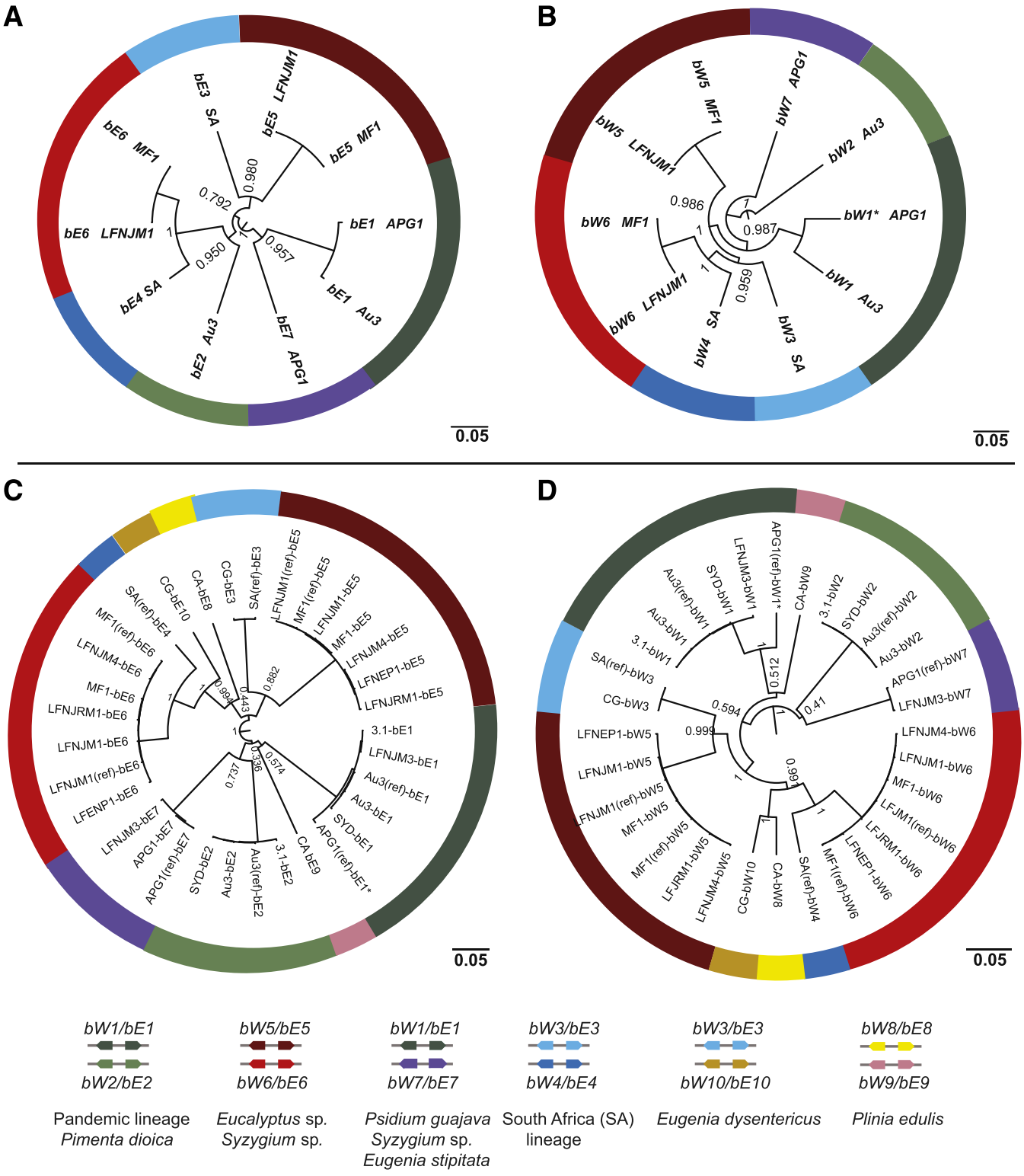

Fig. 1. Bayesian inference genealogical trees reconstructed from *HD* (homeodomain) genes of *Austropuccinia psidii*. Genealogical trees reconstructed from the alignment of two *bE-HD2* (**A and C**) or two *bW-HD1* (**B and D**) alleles per dikaryotic genome assembly of reference isolates (A and B) and with consensus sequences for each allele de novo reconstructed from Oxford Nanopore Technologies long-read amplicons of partial *bE-HD2* (C) and *bW-HD1* (D). Lineage identification is indicated by the combination of different colors in the outer ring of each tree. Reference sequences are indicated with (ref). Bayesian posterior probabilities are shown on the nodes; posterior value of leaves that shared identical sequences are removed. The scale bar represents 0.05 substitutions per site. * indicates highly similar nucleotide sequences that are likely to be functionally identical.

(10 μM), 0.5 μl of Q5 High-Fidelity DNA Polymerase (New England Biolabs), 23.5 μl of NFW, and 5 μl (up to 50 ng) of template DNA. The PCR amplification was performed using the following conditions: initial denaturation at 98°C for 30 s, followed by a touch-down phase of 10 cycles consisting of 98°C for 10 s, 65 to 61°C for 20 s (decreasing by 1°C per cycle), and 72°C for 90 s. This was followed by 25 cycles of 98°C for 10 s, 61°C for 20 s, and 72°C for 90 s. The reaction was completed with a final extension at 72°C for 2 min. PCR products were visualized on 2% agarose gel stained with SYBR Safe (Thermo Fisher Scientific).

For amplifying the additional SOG markers, the reaction mixture, with a final volume of 25 μl, included 5 μl of 5× reaction buffer (New England Biolabs), 5 μl of Q5 GC enhancer, 0.25 μl of bovine serum albumin, 0.5 μl of dNTPs (10 mM), 2.5 μl of each primer (10 μM), 0.25 μl of Q5 High-Fidelity DNA Polymerase (New England Biolabs), 4 μl of NFW, and 5 μl of template DNA. The PCR amplification had an initial denaturation step at 98°C for 30 s, followed by 35 cycles of denaturation at 98°C for 30 s, annealing at 64°C for 20 s, and extension at 72°C for 1 min, with a final extension step at a 72°C for 5 min. PCR products were visualized on 2% agarose gel stained with SYBR Safe (Thermo Fisher Scientific).

ONT sequencing

For Oxford Nanopore sequencing, libraries were generated following manufacturer instructions for V14 Ligation Sequencing of amplicons (Native Barcoding Kit V14 96 - SQK-NBD114.96) with modifications as follows. An initial bead clean step was performed using 1.2 × of 2% Sera-Mag beads to purify the PCR product and 200 fmol of clean DNA carried through to end-prep reaction (Hall et al. 2023). The end-prep reaction was incubated at 20°C and then 65°C for 15 min to maximize yield. One microliter of the end-prepped DNA was barcoded with 1 μl of Nanopore Native Barcode using 5 μl of Blunt/TA Ligase Master Mix (New England Biolabs) in total reaction volume of 10 μl for 20 min at 20°C. The reaction was stopped by adding 1 μl of EDTA to each ligation reaction. The individually barcoded PCR amplicons were pooled and bead cleaned with 0.6 × volume 2% Sera-Mag beads and two washes of 70% ethanol. The pool of barcoded PCR amplicons was eluted in 21 μl of NFW. Library preparation was completed according to the manufacturer's protocol. Twenty femtomoles of the barcoded library was loaded on a MinION R10.4.1 Flowcell (FLO-MIN114) and sequencing was run using a MinION Mk1B sequencing device. Basecalling was performed with Guppy v. 6.4.2 Super High Accuracy mode. All long-read amplicon datasets and consensus sequences were deposited to Zenodo (https://doi.org/10.5281/zenodo.10656657).

De novo reconstruction of *HD* loci and genealogies

A two-step filtering process was implemented on the base-called sequences. In the initial step, sequencing reads were filtered based on their Phred quality scores, with reads having a mean quality score below 15 being removed with Nanofilt v2.6.0 (De Coster et al. 2018). This ensured that the remaining reads had an average per-base accuracy of ≥97%. The second filtering step involved selecting sequencing reads with lengths around the expected amplicon length: 1,500 to 1,800 bp for *bW-HD1* and 1,300 to 1,500 bp for *bE-HD2*.

The VSEARCH orient algorithm (Rognes et al. 2016) was first applied to orient reads according to the reference, and then the clustering algorithm was used to quality control sequencing reads of each sample using a global identity cutoff of 0.85 for clustering. The analysis code is available on Github (https://github.com/TheRainInSpain/Lineage-Specific-Marker.git). And the raw data are available at https://doi.org/10.5281/zenodo.10656657. Geneious software (v.2023.2.1) was used to visualize the forward read consensus sequences (Geneious 2024).

The reconstructed amplicon and reference sequences were aligned (Table 2) with MUSCLE (v.5.1) (Edgar 2004), and genealogical trees were reconstructed using BEAST2 (Bouckaert et al. 2014) with same method described above.

Downstream analysis of secondary loci and genealogies

The base-called sequencing reads were filtered with Nanofilt v.2.6.0 using the same parameter described above. Filtered reads were oriented by applying VSEARCH orient using the pandemic isolate (Au3) target region as reference for each amplicon. The VSEARCH clustering algorithm was used to cluster reads by size with a high identity threshold 0.99. The consensus sequences derived from clusters were aligned to remove duplications. Reads were then mapped back to consensus sequence with BWA-MEM2 for verification. Genealogies of each amplicon were inferred by BEAST2 as described above for *HD* alleles.

To perform principal component analysis (PCA) for differentiating isolates with four identical *bW-HD1* and *bE-HD2* alleles, we included only four secondary loci (OG4974, OG7530, OG9632, and OG9774), which were capable of amplifying at least two alleles per sample. We used the DistanceCalculator from Bio.Phylo to calculate pairwise distances between amplicons. For samples without a reference genome, amplicons were pseudo-phased based on the haplotype of the reference amplicon with the minimum distance to the query. Amplicons belonging to the same isolate were then merged in the following order: OG4974 hapA, OG4974 hapB, OG7530 hapA, OG7530 hapB, OG9632 hapA, OG9632 hapB, OG9774 hapA, and OG9774 hapB. OneHotEncoder (Pedregosa et al. 2011) was utilized to transform the alignment into a numeric array with five categories (A, T, C, G, -). PCA was then applied to reduce dimensionality and visualize the main sources of variance in the data.

Results

Specificity of the diagnostic assay achieved through *HD* loci amplification and ONT sequencing

During the initial phase of primer testing, *HD* amplicon PCRs were performed on positive controls of *A. psidii* (Au3, MF-1, APG1, and LFNJM1) and negative controls with nontarget rust species (*Miyagia pseudosphaeria*, *Puccinia striiformis* f. sp. *tritici*, *P. graminis*, *P. triticina*, and *Thekopsora minima*). In addition, we focused on the individual PCR amplicons (*bW-HD1* and *bE-HD2*) because the amplification of the full-length locus was not robust enough across samples and technical replicates. The sizes of the amplicons were as expected in the positive control samples, being of ~1,600 bp for *bW-HD1*, ~1,400 bp for *bE-HD2*, and ~2,400 kb for the full HD locus (Table 2). In addition, we observed bands of variable sizes in some of our technical repeats of nontarget species. All samples were sequenced with our ONT amplicon sequencing workflow because our assay does not rely exclusively on the PCR amplification but requires that the amplified sequences match the *A. psidii HD* sequences in a genealogical framework.

None of the nontarget species amplicon sequences matched the full-length *A. psidii HD* sequences. For each *A. psidii* isolate, four *HD* alleles (2 × *bW-HD1* and 2 × *bE-HD2*) were reconstructed based on ONT sequencing results, as expected for dikaryotic organisms. Isolates were considered identical if their four *HD* alleles had >99.9% of pairwise identity. The applicability of the lineage diagnostic test was confirmed by comparing the de novo reconstructed consensus sequences derived from ONT amplicon sequencing with the in silico-derived *bW-HD1/bE-HD2* amplicon sequences based on available reference genomes (APG1, MF-1, LFNJM1, Au3, and Apsidii_AM). All de novo reconstructed ONT amplicon sequences clearly grouped with their respective *HD* alleles obtained from reference genomes (Fig. 1A and B; Table 2). Moreover, the reference trees for *bW-HD1* and *bE-HD2* revealed that the Brazilian isolates and the South African isolate carry at least two clearly distinct alleles when compared against the pandemic lineage (Fig. 1A and B), corroborating variations previously described using microsatellite markers (Graça et al. 2013; Roux et al. 2016; Stewart et al. 2018).

Primers targeting the *HD* region distinguished different lineages of *A. psidii*

The designed primers successfully amplified individual *HD* loci of DNA extracted from different sources of field samples, including

Table 3. Classification of secondary diagnostic markers of *Austropuccinia psidii*

	OG4974		OG5363		OG7071		OG7530		OG9632		OG9774	
Isolate code	***hapA***	***hapB***	***hapA***	***hapB***	***hapA***	***hapB***	***hapA***	***hapB***	***hapA***	***hapB***	***hapA***	***hapB***
Genomes												
Au3	OG4974-1	OG4974-2	OG5363-1	OG5363-2	OG7071-1	OG7071-2	OG7530-1	OG7530-2	OG9632-1	OG9632-2	OG9774-1	OG9774-2
MF-1	OG4974-4	OG4974-5	OG5363-4	OG5363-5	OG7071-4	OG7071-5	OG7530-5	OG7530-6	OG9632-3	OG9632-4	OG9774-2	OG9774-3
APG1 (GM1)	OG4974-3	OG4974-6	OG5363-3	OG5363-6	OG7071-3	OG7071-1	OG7530-3	OG7530-4	OG9632-5	OG9632-7	OG9774-4	OG9774-5
LFNJM1	OG4974-4	OG4974-5	OG5363-4	OG5363-5	OG7071-4	OG7071-5	OG7530-5[a]	OG7530-6	OG9632-3	OG9632-4	OG9774-2	OG9774-3
Isolates (single-pustule)												
Au3[b]	OG4974-1	OG4974-2	OG5363-1	OG5363-2	OG7071-1	OG7071-2	OG7530-1	OG7530-2	OG9632-1	OG9632-2	OG9774-1	OG9774-2
MF-1[b]	OG4974-4	OG4974-5	OG5363-4	OG5363-5	OG7071-4	OG7071-5	OG7530-5	OG7530-6	OG9632-3	OG9632-4	OG9774-2	OG9774-3
APG1 (GM1)[b]	OG4974-3	OG4974-6	OG5363-3	OG5363-6	OG7071-3	OG7071-1	OG7530-3	OG7530-4	OG9632-5	OG9632-7	OG9774-4	OG9774-5
LFNJM1[b]	OG4974-4	OG4974-5	OG5363-4	OG5363-5	OG7071-4	OG7071-5	OG7530-5[a]	OG7530-6	OG9632-3	OG9632-4	OG9774-2	OG9774-3
LFNJM3	OG4974-7	OG4974-6[a]	OG5363-4[a]	NA	OG7071-6	OG7071-6	OG7530-2	OG7530-4	OG9632-1[a]	OG9632-8	OG9774-4	OG9774-5
LFNJM4	OG4974-4	OG4974-5[a]	OG5363-4	OG5363-5	OG7071-4	OG7071-5	OG7530-5	OG7530-6	OG9632-3	OG9632-4	OG9774-2	OG9774-3
LFNJRM1	OG4974-4	OG4974-5	OG5363-4	OG5363-5	OG7071-4	OG7071-5	OG7530-5[a]	OG7530-6	OG9632-3	OG9632-4	OG9774-2	OG9774-3
Populations (urediniospores/field samples)												
CA	OG4974-1[a]	OG4974-8	OG5363-7	OG5363-8	OG7071-7	OG7071-2	OG7530-1/OG7530-2	OG7530-7	OG9632-9	OG9632-6	OG9774-1	OG9774-3
CG	OG4974-5[a]	OG4974-5	OG5363-5[a]	OG5363-5	NA	OG7071-5	OG7530-2	OG7530-2	OG9632-8	OG9632-4	OG9774-3	OG9774-3
Populations (infected leaves/field samples)												
LFNEP1	OG4974-4	OG4974-5	OG5363-4	OG5363-5	OG7071-4	OG7071-5	OG7530-5	OG7530-6	OG9632-3	OG9632-4	OG9774-2	OG9774-3
3.1	OG4974-1	OG4974-2	OG5363-1	OG5363-2	OG7071-1	OG7071-2	OG7530-1	OG7530-2	OG9632-1	OG9632-2	OG9774-1[a]	OG9774-2
SYD	OG4974-1	OG4974-2	OG5363-1	OG5363-2	OG7071-1	OG7071-2	OG7530-1	OG7530-2	OG9632-1	OG9632-2	OG9774-1[a]	OG9774-2

[a] Allele differs by at least 3 base pairs from other alleles.
[b] *A. psidii* rust isolates used to confirm the specificity of the designed primers.

urediniospores (CA and CG) and infected leaf material (LFNEP1, SYD, and 3.1) (Table 2). As observed previously, the full *HD* locus amplification was not possible for the APG1 isolate and the field samples (Table 2). The reconstructed *bW-HD1/bE-HD2* amplicons and reference sequences were aligned. Sequences with a pairwise identity >99.9% were considered the same allele across different isolates. Our results revealed that isolate SYD and isolate 3.1, collected from field samples in Australia in 2022 and Brazil in 2023, most likely belong to the Au3 group, corresponding to the pandemic lineage because all four *HD* alleles clearly grouped with those derived from the pandemic reference isolate (Fig. 1C and D). In contrast, other isolates collected from Brazil belong to different lineages having at least two different *HD* alleles from the pandemic lineage (Fig. 1C and D).

Isolates LFNJM1, LFNJM4, LFNNJRM1, LFNEP1, and MF-1 belong to the MF-1/LFNJM1 group, which includes isolates that infect *Eucalyptus* sp., *S. jambos*, *S. samarangense*, and *Eugenia stipitata.* Isolates APG1 and LFNJM3 belong to the APG1 group, which infects *P. guajava* and *S. jambos.* Isolates CG and CA did not group with other isolates (Fig. 1C and D).

Notably, the 3.1 leaf sample collected from Brazil in 2023 showed identical *bW-HD1* and *bE-HD2* alleles to the pandemic lineage, necessitating further testing with additional secondary diagnostic amplicons.

Secondary diagnostic amplicons allow more sensitive lineage calling

We aimed to further differentiate samples that share identical *HD* alleles, for example, the Au3 group, MF1/LFNJM1 group, and APG1 group. For this purpose, we identified six additional secondary diagnostic amplicons that target highly variable regions of SOGs (Table 3). Primer pairs for amplicons OG4974, OG9632, and OG9774 amplified two alleles for all samples. Other amplicons recovered two alleles in all samples, except for OG7530, which amplified three alleles for CG, OG5363, which amplified only one allele for LFNJM3, and OG7071, which amplified one allele for CG. The genealogical trees show that samples that shared identical *HD* alleles have similar alleles of the additional tested amplicons (Supplementary Figs. S2A to F, S3, and S4). However, a deletion specific to the OG9774 allele of Au3 and SYD, and an insertion of a tandem repeat specific to the OG7530 allele of MF1, LFNJM4, and LFENP1, allowed further differentiation of samples that share identical *HD* alleles (Supplementary Fig. S4A and B).

To generate the PCA plot, OG4974, OG7530, OG9632, and OG9774, which amplified at least two alleles per sample, were selected. The OG7530 amplicon amplified three alleles for CG, with OG7530-7 being the best supported by the sequencing reads. In contrast, OG7530-2 and OG7530-1 had fewer reads, but their read counts were similar. Therefore, we used two combinations of OG7530 for the CG isolate: OG7530-2 + OG7530-7 and OG7530-1 + OG7530-7. The PCA plot indicates that SYD belongs to the same lineage as the pandemic lineage Au3. Except for OG7530, the other five secondary diagnostic amplicons of the leaf sample 3.1 were identical to the pandemic lineage. The amplicon for OG7530 distinguished the leaf sample 3.1 from the pandemic biotype in the PCA analysis (Supplementary Figs. S3 and S4). This suggests that the leaf sample 3.1 is derived from an isolate that is likely closely related to or the same biotype as the pandemic lineage. CA, LFNJM3, and CG, which have a unique combination of *HD* alleles, are genetically distinct from all isolates with reference genomes including Au3 (Fig. 2A and B). Among the samples with the combinations of *bW5-HD1/bE5-HD2* and *bW6-HD1/bE6-HD2* (MF-1/LFNM1 group), LFNJM1 and LFNJRM1 belong to one lineage, whereas LFNEP1 and MF-1 belong to another. LFNJM4 was derived from a different lineage than the other samples.

Discussion

Traditionally, *A. psidii* lineages have been identified using microsatellite markers (Graça et al. 2013; Kaur et al. 2015; Roux et al. 2016; Stewart et al. 2018). In this study, a diagnostic assay targeting the *bW-HD1*, *bE-HD2*, and six additional SOGs of *A. psidii*, coupled with ONT sequencing, was developed. This method successfully amplified diverse copies of all eight loci from *A. psidii* isolates collected in Australia and Brazil and is predicted to work for the South African isolate.

Ten alleles for *bW-HD1* and *bE-HD1* were identified within the isolates used in this study (Fig. 1, Table 2). These findings are consistent with the allelic diversity observed in the other four rust species, *Puccinia coronata* f. sp. *avenaae*, *P. graminis* f. sp. *tritici*, *P. triticina*, and *P. striiformis* f. sp. *tritici*, where estimates range between 6 and 12 alleles for *bW-HD1* and *bE-HD2* (Henningsen et al. 2024; Holden et al. 2023; Luo et al. 2024). Although these allele counts likely underestimate the total circulating *HD* alleles within the global *A. psidii* population, our results support previous findings related to host specialization.

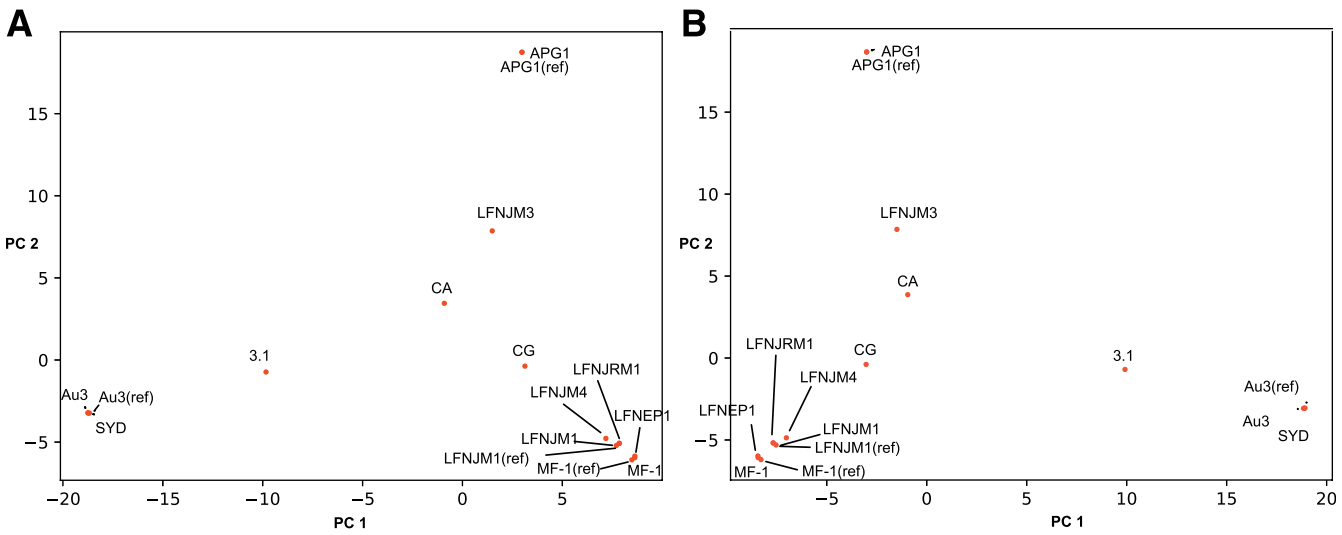

Fig. 2. Principal component analysis (PCA) of four amplicons (OG4974, OG7530, OG9632, and OG9774) shows distinguishable differences between samples. Each point represents a single sample, and the spatial relationships between points indicate similarities or differences within alignments. **A,** PCA plot of alignment with CA has combination of OG7530-1 and OG7530-7. **B,** PCA plot of alignment with CA has combination of OG7530-2 and OG7530-7. 3.1, which has identical *HD* alleles as the pandemic lineage segregate from the pandemic lineage sample, reference, and SYD isolate. JM1 and JRM1 clustered as one point, whereas LFNEP1 and MF1 clustered into another. JM4 was derived from a different lineage than the other samples.

In our study, the combination of alleles *bW1/2-HD1* and *bE1/2-HD2* was found in the isolate Au3 (positive control), SYD (field sample), and only one Brazilian leaf sample (3.1). This Au3 belongs to the pandemic biotype lineage (Graça et al. 2013; Kaur et al. 2015; Roux et al. 2016; Stewart et al. 2018), which was initially associated with the emergence of myrtle rust across the globe, including Australia, where this genetic group appears to be the only biotype present so far (Sandhu et al. 2016; Stewart et al. 2018). The pandemic biotype of *A. psidii* was previously reported in Colombia, South America (Granados et al. 2017); however, as far as we know, this represents the first report of this biotype or a very closely related lineage in Brazil. Further support for this diagnosis should include the isolation of single-pustule cultures from nearby infected plant material and whole-genome sequencing and analysis. The divergence of alleles observed among isolates from *Eucalyptus* sp./*S. jambos* and *P. guajava* aligns with earlier observations of distinct genetic groups specialized to different hosts in South America (Graça et al. 2013; Stewart et al. 2018). Recently, Morales et al. (2024) further elucidated this specialization for isolates LFNJM1 (from *S. jambos*) and APG1 (from *P. guajava*) to their respective original hosts; these are the same isolates used as positive controls in this study (Table 2). As in other systems like *Puccinia striiformis* f. sp. *tritici* and *Puccinia coronata* f. sp. *avenae*, there have been indications that *HD* alleles can be shared between populations (Henningsen et al. 2024; Holden et al. 2023).

The genealogical tree of de novo reconstructed amplicons confirmed the biological expectation of lineage-specific variation among isolates originating from single spores, field samples from different hosts, and distinct geographic locations. The isolate collected from field samples in Australia had all eight alleles matching to the pandemic lineage isolate Au3, whereas in Brazil, the center of origin of the disease, there was a strong association of *HD* allele status with their original host species, as previously observed (Graça et al. 2013; Morales et al. 2024; Stewart et al. 2018).

Using all eight diagnostic markers, we can clearly differentiate nonpandemic samples from the pandemic reference isolate (Au3) and Australian field samples. Hence, our new diagnostic protocol serves as a valuable tool in detecting new incursions of the pathogen in regions where a single lineage is present, as for example in Australia where only a single incursion has been reported to date. Further, comparing marker allele identities with known reference sequences could link novel incursions with related populations in source regions. This could help in identifying risks in import pathways of this exotic pathogen and improving risk mitigation strategies. In addition, the assay could potentially detect recombination between populations if purified single-pustule isolates were analyzed. In the future, we anticipate that the diagnostic test can be refined to detect urediniospores of *A. psidii* from complex samples derived from air sampling or mixed infections to enable structured targeted surveillance of this pathogen on the ground.

Acknowledgments

The authors thank Danièle Giblot-Ducray and Kelly Hill for the critical feedback and support, Maria Carolina Quecine for providing the MF-1 isolate of *A. psidii*, and Tuan Duong for sharing WGS data of SA isolate of *A. psidii*. We gratefully acknowledge the computational resources provided by the National Computational Infrastructure (NCI) and ANU Merit Allocation Scheme (ANUMAS).

Literature Cited

Ahmed, M. B., dos Santos, K. C. G., Sanchez, I. B., Petre, B., Lorrain, C., Plourde, M. B., Duplessis, S., Desgagné-Penix, I., and Germain, H. 2018. A rust fungal effector binds plant DNA and modulates transcription. Sci. Rep. 8:14718.

Baskarathevan, J., Taylor, R. K., Ho, W., McDougal, R. L., Shivas, R. G., and Alexander, B. J. R. 2016. Real-time PCR assays for the detection of *Puccinia psidii*. Plant Dis. 100:617-624.

Beenken, L. 2017. *Austropuccinia*: A new genus name for the myrtle rust *Puccinia psidii* placed within the redefined family Sphaerophragmiaceae (Pucciniales). Phytotaxa 297:53-61.

Bouckaert, R., Heled, J., Kühnert, D., Vaughan, T., Wu, C.-H., Xie, D., Suchard, M. A., Rambaut, A., and Drummond, A. J. 2014. BEAST 2: A software platform for Bayesian evolutionary analysis. PLoS Comput. Biol. 10:e1003537.

Boufleur, T. R., Morales, J. V. P., Martins, T. V., Gonçalves, M. P., Júnior, N. S. M., and Amorim, L. 2023. A diagnostic guide for myrtle rust. Plant Health Prog. 24:242-251.

Carnegie, A. J., and Giblin, F. R. 2014. *Austropuccinia psidii* (Myrtle Rust). Invasive Species Compendium. CABI, Wallingford, U.K. https://www.cabi.org/isc/datasheet/45846

Carnegie, A. J., Lidbetter, J. R., Walker, J., Horwood, M. A., Tesoriero, L., Glen, M., and Priest, M. J. 2010. *Uredo rangelii*, a taxon in the guava rust complex, newly recorded on Myrtaceae in Australia. Australas. Plant Pathol. 39:463-466.

Chock, M. K. 2020. The global threat of Myrtle rust (*AUSTROPUCCINIA psidii*): Future prospects for control and breeding resistance in susceptible hosts. Crop Prot. 136:105176.

Coelho, M. A., Bakkeren, G., Sun, S., Hood, M. E., and Giraud, T. 2017. Fungal sex: The Basidiomycota. Microbiol. Spectr. 5. https://doi.org/10.1128/microbiolspec.funk-0046-2016

Cuomo, C. A., Bakkeren, G., Khalil, H. B., Panwar, V., Joly, D., Linning, R., Sakthikumar, S., Song, X., Adiconis, X., Fan, L., Goldberg, J. M., Levin, J. Z., Young, S., Zeng, Q., Anikster, Y., Bruce, M., Wang, M., Yin, C., McCallum, B., Szabo, L. J., Hulbert, S., Chen, X., and Fellers, J. P. 2017. Comparative analysis highlights variable genome content of wheat rusts and divergence of the mating loci. G3 7:361-376.

DAFF. 2023. Myrtle Rust. Department of Agriculture, Fisheries and Forestry (DAFF), Australia. https://www.agriculture.gov.au/biosecurity-trade/pests-diseases-weeds/plant/myrtle-rust (accessed 21 August 2024).

De Coster, W., D'Hert, S., Schultz, D. T., Cruts, M., and Van Broeckhoven, C. 2018. NanoPack: Visualizing and processing long-read sequencing data. Bioinformatics 34:2666-2669.

dos Santos, A. P., Lanças Gomes, R., Furtado, E. L., and de Souza Passos, J. R. 2020. Quantifying losses in productivity by the rust in eucalypt plantations in Brazil. For. Ecol. Manag. 468:118170.

Drummond, A. J., and Rambaut, A. 2009. Bayesian evolutionary analysis by sampling trees. Pages 564-591 in: The Phylogenetic Handbook: A Practical Approach to Phylogenetic Analysis and Hypothesis Testing. P. Lemey, M. Salemi, and A.-M. Vandamme, eds. Cambridge University Press, Cambridge, U.K.

Edgar, R. C. 2004. MUSCLE: Multiple sequence alignment with high accuracy and high throughput. Nucleic Acids Res. 32:1792-1797.

Edwards, R. J., Dong, C., Park, R. F., and Tobias, P. A. 2022. A phased chromosome-level genome and full mitochondrial sequence for the dikaryotic myrtle rust pathogen, *Austropuccinia psidii*. bioRxiv. https://doi.org/10.1101/2022.04.22.489119

Emms, D. M., and Kelly, S. 2019. OrthoFinder: Phylogenetic orthology inference for comparative genomics. Genome Biol. 20:238.

Ferrarezi, J. A., McTaggart, A. R., Tobias, P. A., Hayashibara, C. A. A., Degnan, R. M., Shuey, L. S., Franceschini, L. M., Lopes, M. S., and Quecine, M. C. 2022. *Austropuccinia psidii* uses tetrapolar mating and produces meiotic spores in older infections on *Eucalyptus grandis*. Fungal Genet. Biol. 160:103692.

FigTree. 2016. http://tree.bio.ed.ac.uk/software/figtree/ (accessed 17 November 2023).

Geneious. 2024. From Data to Discovery—Faster. https://www.geneious.com

Gonçalves, M. P., Nogueira Júnior, A. F., Ribeiro, R. V., and Amorim, L. 2022. Monocyclic components and photosynthetic damage caused by myrtle rust in guava leaves. Phytopathology 112:1467-1475.

Graça, R. N., Ross-Davis, A. L., Klopfenstein, N. B., Kim, M.-S., Peever, T. L., Cannon, P. G., Aun, C. P., Mizubuti, E. S. G., and Alfenas, A. C. 2013. Rust disease of eucalypts, caused by *Puccinia psidii*, did not originate via host jump from guava in Brazil. Mol. Ecol. 22:6033-6047.

Granados, G. M., McTaggart, A. R., Barnes, I., Rodas, C. A., Roux, J., and Wingfield, M. J. 2017. The pandemic biotype of *Austropuccinia psidii* discovered in South America. Australas. Plant Pathol. 46:267-275.

Hall, R. N., Jones, A., Crean, E., Marriott, V., Pingault, N., Marmor, A., Sloan-Gardner, T., Kennedy, K., Coleman, K., Johnston, V., and Schwessinger, B. 2023. Public health interventions successfully mitigated multiple incursions of SARS-CoV-2 Delta variant in the Australian Capital Territory. Epidemiol. Infect. 151:e30.

Henningsen, E. C., Lewis, D., Nazareno, E., Huang, Y.-F., Steffenson, B. J., Boesen, B., Kianian, S. F., Stone, E., Dodds, P. N., Sperschneider, J., and Figueroa, M. 2024. A high-resolution haplotype pangenome uncovers somatic hybridization, recombination and intercontinental migration in oat crown rust. bioRxiv. https://doi.org/10.1101/2024.03.27.583983

Holden, S., Bakkeren, G., Hubensky, J., Bamrah, R., Abbasi, M., Qutob, D., de Graaf, M.-L., Kim, S. H., Kutcher, H. R., McCallum, B. D., Randhawa, H. S., Iqbal, M., Uloth, K., Burlakoti, R. R., and Brar, G. S. 2023. Uncovering the history of recombination and population structure in western Canadian stripe rust populations through mating type alleles. BMC Biol. 21:233.

Hussain, K. K., Malavia, D., Johnson, E. M., Littlechild, J., Winlove, C. P., and Vollmer, F., Gow, N. A. R. 2020. Biosensors and diagnostics for fungal detection. J. Fungi 6:349.

Hyde, K. D., Al-Hatmi, A. M. S., Andersen, B., Boekhout, T., Buzina, W., Dawson, T. L., Jr., Eastwood, D. C., Jones, E. B. G., de Hoog, S., Kang, Y., Longcore, J. E., McKenzie, E. H. C., Meis, J. F., Pinson-Gadais, L.,

Rathnayaka, A. R., Richard-Forget, F., Stadler, M., Theelen, B., Thongbai, B., and Tsui, C. K. M. 2018. The world's ten most feared fungi. Fungal Divers. 93:161-194.

IPPC. 2018. DP 26: *Austropuccinia psidii*. Food and Agriculture Organization of the United Nations, Rome, Italy.

Johnson, M., Zaretskaya, I., Raytselis, Y., Merezhuk, Y., McGinnis, S., and Madden, T. L. 2008. NCBI BLAST: A better web interface. Nucleic Acids Res. 36:W5-W9.

Jukes, T. H., and Cantor, C. R. 1969. Evolution of protein molecules. Pages 21-132 in: Mammalian Protein Metabolism. Vol. 3. H. N. Munro, ed. Academic Press, New York.

Katoh, K., and Standley, D. M. 2013. MAFFT multiple sequence alignment software version 7: Improvements in performance and usability. Mol. Biol. Evol. 30:772-780.

Kaur, S., Panesar, P. S., Bera, M. B., and Kaur, V. 2015. Simple sequence repeat markers in genetic divergence and marker-assisted selection of rice cultivars: A review. Crit. Rev. Food Sci. Nutr. 55:41-49.

Luo, Z., McTaggart, A., and Schwessinger, B. 2024. Genome biology and evolution of mating-type loci in four cereal rust fungi. PLoS Genet. 20: e1011207.

Makinson, R. O., Pegg, G. S., and Carnegie, A. J. 2020. Myrtle Rust in Australia–A National Action Plan. Australian Plant Biosecurity Science Foundation, Canberra, Australia.

McTaggart, A. R., Duong, T. A., Le, V. Q., Shuey, L. S., Smidt, W., Naidoo, S., Wingfield, M. J., and Wingfield, B. D. 2018. Chromium sequencing: The doors open for genomics of obligate plant pathogens. Biotechniques 65:253-257.

Morales, J. V. P., Boufleur, T. R., Gonçalves, M. P., Parisi, M. C. M., Loehrer, M., Schaffrath, U., and Amorim, L. 2024. Differential aggressiveness of *Austropuccinia psidii* isolates from guava and rose apple upon cross-inoculation. Plant Pathol. 73:915-923.

Pedregosa, F., Varoquaux, G., Gramfort, A., Michel, V., Thirion, B., Grisel, O., Blondel, M., Prettenhofer, P., Weiss, R., Dubourg, V., Vanderplas, J., Passos, A., Cournapeau, D., Brucher, M., Perrot, M., and Duchesnay, É. 2011. Scikit-learn: Machine learning in Python. J. Machine Learn. Res. 12:2825-2830.

Quick, J., Grubaugh, N. D., Pullan, S. T., Claro, I. M., Smith, A. D., Gangavarapu, K., Oliveira, G., Robles-Sikisaka, R., Rogers, T. F., Beutler, N. A., Burton, D. R., Lewis-Ximenez, L. L., de Jesus, J. G., Giovanetti, M., Hill, S. C., Black, A., Bedford, T., Carroll, M. W., Nunes, M., Alcantara, L. C., Jr., Sabino, E. C., Baylis, S. A., Faria, N. R., Loose, M., Simpson, J. T., Pybus, O. G., Andersen, K. G., and Loman, N. J. 2017. Multiplex PCR method for MinION and Illumina sequencing of Zika and other virus genomes directly from clinical samples. Nat. Protoc. 12:1261-1276.

Rice, P., Longden, I., and Bleasby, A. 2000. EMBOSS: The European molecular biology open software suite. Trends Genet. 16:276-277.

Rognes, T., Flouri, T., Nichols, B., Quince, C., and Mahé, F. 2016. VSEARCH: A versatile open source tool for metagenomics. PeerJ 4:e2584.

Roux, J., Granados, G. M., Shuey, L., Barnes, I., Wingfield, M. J., and McTaggart, A. R. 2016. A unique genotype of the rust pathogen, *Puccinia psidii*, on Myrtaceae in South Africa. Australas. Plant Pathol. 45:645-652.

Sandhu, K. S., Karaoglu, H., Zhang, P., and Park, R. F. 2016. Simple sequence repeat markers support the presence of a single genotype of *Puccinia psidii* in Australia. Plant Pathol. 65:1084-1094.

Sievers, F., Wilm, A., Dineen, D., Gibson, T. J., Karplus, K., Li, W., Lopez, R., McWilliam, H., Remmert, M., Söding, J., Thompson, J. D., and Higgins, D. G. 2011. Fast, scalable generation of high-quality protein multiple sequence alignments using Clustal Omega. Mol. Syst. Biol. 7:539.

Simpson, J. A., Thomas, K., and Grgurinovic, C. A. 2006. Uredinales species pathogenic on species of Myrtaceae. Australas. Plant Pathol. 35:549-562.

Stewart, J. E., Ross-Davis, A. L., Graça, R. N., Alfenas, A. C., Peever, T. L., Hanna, J. W., Uchida, J. Y., Hauff, R. D., Kadooka, C. Y., Kim, M.-S., Cannon, P. G., Namba, S., Simeto, S., Pérez, C. A., Rayamajhi, M. B., Lodge, D. J., Arguedas, M., Medel-Ortiz, R., López-Ramirez, M. A., Tennant, P., Glen, M., Machado, P. S., McTaggart, A. R., Carnegie, A. J., and Klopfenstein, N. B. 2018. Genetic diversity of the myrtle rust pathogen (*Austropuccinia psidii*) in the Americas and Hawaii: Global implications for invasive threat assessments. For. Pathol. 48:e12378.

Wilson, A. M., Godlonton, T., van der Nest, M. A., Wilken, P. M., Wingfield, M. J., and Wingfield, B. D. 2015. Unisexual reproduction in *Huntiella moniliformis*. Fungal Genet. Biol. 80:1-9.

Winter, G. 1884. Repertorium. Rabenhorstii fungi europaei et extraeuropaei exsiccati cura Dr. G. Winter, Centuria XXXI et XXXII. Hedwigia 23:164-172.